JMB
Journal of Microbiology and Biotechnology

Online ISSN : 1738-8872
Pirnt ISSN : 1017-7825

JMB Papers in Press. First Published online Mar 31, 2015
DOI: 10.4014/jmb.1503.03031

Manuscript Number: JMB15-03031

Title: Molecular Analysis of Promoter and Intergenic Region Attenuator of the Vibrio vulnificus prx1ahpF Operon

Article Type: Research article

Keywords: Vibrio vulnificus, peroxiredoxin, alkyl hydroperoxide reductase, transcriptional attenuation

Molecular Analysis of Promoter and Intergenic Region Attenuator of the *Vibrio vulnificus prx*1*ahpF* Operon

Hyun Sung Lee[2], Jong Gyu Lim[1], Kook Han[3], Younghoon Lee[3], and Sang Ho Choi[1]*

[1]National Research Laboratory of Molecular Microbiology and Toxicology, Department of Agricultural Biotechnology, and Center for Food Safety and Toxicology, Seoul National University, Seoul 151-921, South Korea

[2]Korea Food Research Institute, Seongnam 463-746, South Korea

[3]Department of Chemistry, Korea Advanced Institute of Science and Technology (KAIST), Daejeon 305-701, South Korea

Running Title: Regulation of *V. vulnificus prx*1*ahpF* operon

*Corresponding author:
Sang Ho Choi
Department of Agricultural Biotechnology
Seoul National University
Seoul, 151-921, South Korea
Tel; +82-2-880-4857, Fax; 82-2-873-5095
E-mail: choish@snu.ac.kr

Abstract

Prx1, an AhpF-dependent 2-Cys peroxiredoxin (Prx), was previously identified in *Vibrio vulnificus*, a facultative aerobic pathogen. In the present study, transcription of the *V. vulnificus prx*1*ahpF* genes, which are adjacently located on the chromosome, was evaluated by analyzing the promoter and intergenic region of the two genes. Northern blot analyses revealed that transcription of *prx*1*ahpF* results in two transcripts, the *prx*1 and *prx*1*ahpF* transcripts. Primer extension analysis and a point mutational analysis of the promoter region showed that the two transcripts are generated from a single promoter. In addition, the 3' end of *prx*1 transcript at the *prx*1*ahpF* intergenic region was determined by a 3'RACE assay. These results suggested that the *prx*1*ahpF* genes are transcribed as an operon, and the *prx*1 transcript was produced by transcriptional termination in the intergenic region. RNA secondary structure prediction of the *prx*1*ahpF* intergenic region singled out a stem-loop structure without poly(U) tract, and a deletion analysis of the intergenic region showed that the atypical stem-loop structure acts as the transcriptional attenuator to result in the *prx*1 and *prx*1*ahpF* transcripts. Combined results demonstrated that the differential expression of *prx*1 and *ahpF* is accomplished by the *cis*-acting transcriptional attenuator located between the two genes and thereby leads to the production of high level of Prx1 and low level AhpF.

Keywords : *Vibrio vulnificus*, peroxiredoxin, alkyl hydroperoxide reductase, transcriptional attenuation

Introduction

Bacteria continually encounter toxic reactive oxygen species (ROS), such as superoxide anion ($O_2^{-}\cdot$), hydrogen peroxide (H_2O_2), and hydroxyl radical (·OH), that are generated by incomplete reduction of oxygen during respiration and aerobic metabolism [29, 31]. Oxidative stress caused by increased levels of ROS can lead to the damage of cellular components including metal centers, protein, DNA, and membrane lipid [29, 31]. Particularly, pathogenic bacteria have to cope with oxidative stress imposed by immune systems to survive host environments and in turn to ensure developing illness [8, 21, 25]. Therefore, pathogens have evolved sophisticated mechanisms to overcome oxidative stress, and the mechanisms are closely linked to their virulence [8, 25].

The mechanisms of bacterial defense against oxidative stress include highly specific and effective antioxidant enzymes such as superoxide dismutase, catalase, and peroxiredoxin (Prx) [6, 11]. Among these, Prxs are a ubiquitous family of cysteine-based peroxidases and catalyze the reduction of peroxides such as H_2O_2 and organic hydroperoxide [6, 27]. Typical 2-Cys Prxs, the largest group of Prxs, have two conserved catalytic cysteines, peroxidatic and resolving cysteines. Peroxidatic cysteine reacts with peroxides and forms a cysteine sulfenic acid intermediate, which is followed by the formation of an intermolecular disulfide bond with resolving cysteine from another subunit. Disulfide-bonded 2-Cys Prxs are subsequently reduced and reactivated by thiol-containing reductants such as thioredoxin (Trx) and alkyl hydroperoxidase subunit F (AhpF) [10].

AhpC (alkyl hydroperoxidase subunit C), originally identified from *Escherichia coli* and *Salmonella typhimurium*, is one of the best characterized 2-Cys Prxs and utilizes AhpF as a

reductant to compose an NADH-dependent peroxidase system [5, 12, 30]. AhpF is a flavoprotein with NADH:disulfide oxidoreductase activity and restores the disulfide bond in AhpC to reduced form by transferring electrons from NADH to AhpC [6]. In most cases, the *ahpF* gene is located adjacent downstream of the *ahpC* gene on the chromosome and is co-transcribed with *ahpC* as an operon [6]. The expressions of *ahpCF* are activated by OxyR which is a central regulator of the oxidative stress response when exposed to exogenous oxidants in a number of bacteria [7]. However, studies about the exact molecular mechanisms of *ahpCF* transcription are still limited [6].

In a facultative aerobic pathogen *Vibrio vulnificus*, a 2-Cys Prx, which is highly homologous to other bacterial Prxs such as *E. coli* AhpC (78% identity in amino acid sequences) was previously identified and designated as Prx1 (formerly *V. vulnificus* AhpC) [2]. Prx1, forming an NADH-dependent peroxide reductase system with AhpF, is effective at decomposing large amounts of peroxides rapidly and contributes to not only the growth and survival of the pathogen under exogenous oxidative stress but also virulence in mice [2, 3]. The *V. vulnificus ahpF* gene is located downstream of the *prx*1 gene and the *prx*1*ahpF* transcription is positively regulated by *V. vulnificus* OxyR1, a homologue of *E. coli* OxyR only in cells exposed to high levels of exogenous H_2O_2, to result in the *prx*1 and *prx*1*ahpF* transcripts [16]. However, molecular analysis of the *prx*1*ahpF* transcription has not yet been experimentally verified. Here, we provided molecular genetic evidence that the *V. vulnificus prx*1*ahpF* genes are transcribed as an operon from a single promoter, and a stem-loop structure located between the two genes attenuates the transcription to result in a high level of *prx*1 transcript and a low level of *prx*1*ahpF* transcript. Finally, the physiological role of differential expression of *prx*1 and *ahpF* was discussed.

Materials and Methods

Strains, plasmids, and culture conditions

The strains and plasmids used in this study are listed in Table 1. Unless noted otherwise, the *V. vulnificus* strains were grown aerobically in Luria-Bertani (LB) medium supplemented with 2.0% (w/v) NaCl (LBS) at 30°C.

Generation of *ahpF* mutant

To inactivate *ahpF in vitro*, a unique BamHI site was introduced into the open reading frame (ORF) of *ahpF* using the PCR-mediated linker-scanning mutation method as described previously [16]. Briefly, pairs of primers AHPF0801 and AHPF0802 for amplification of the 5' amplicon or AHPF0803 and AHPF0804 for amplification of the 3' amplicon were designed and used (Table 2). The *ahpF* with BamHI site was amplified by PCR using the mixture of both amplicons as the template and AHPF0801 and AHPF0804 as primers. The *ahpF*::*nptI* was constructed by insertion of a 1.2-kb *nptI* DNA conferring resistance to kanamycin [26] into the BamHI site of the PCR products, and ligated with SacI-SpeI-digested pDM4 [23] to form pWK0805 (Table 1). The *E. coli* SM10 λ *pir, tra* strain [22] containing pWK0805 was used as a conjugal donor to *V. vulnificus* MO6-24/O to generate the *ahpF* mutant BK081 (Table 1). The conjugation and isolation of the transconjugants were conducted as previously described [16].

RNA purification and transcript analysis

Total cellular RNAs from the *V. vulnificus* strains grown to an A_{600} of 0.5 were isolated using an RNeasy® Mini Kit (Qiagen, Valencia, CA) [19]. When necessary, the strains were exposed to 250 μM H_2O_2 (Sigma, St. Louis, MO) for 30 min and then harvested. For Northern blot

analysis, reactions were performed according to standard procedures [28] with 15 μg of RNA. The DNA probes, PRX1P and AHPFP, were prepared respectively by labelling DNA fragments containing the *prx*1 and *ahpF* coding regions with [α-32P]-dCTP, and used for hybridization as previously described [16]. For primer extension analysis, a 24-base oligonucleotide primer PRX1-PE02 (Table 2) complementary to the coding region of *prx*1 was end-labelled with [γ-32P]-ATP and added to the RNA. The primer was then extended with SuperScript II RNase H− reverse transcriptase (Invitrogen, Carlsbad, CA). The cDNA products were purified and resolved on a sequencing gel alongside sequencing ladders generated from pSS1050 with the same primer. The plasmid pSS1050 was constructed by cloning the 410-bp *prx*1 upstream region extending from −271 to +139, amplified by PCR using a pair of primers PRX1-PE01 and -PE02 (Table 2), into pGEM-T Easy (Promega, Madison, WI). The Northern blots and primer extension gels were visualized using a phosphorimage analyzer (BAS1500, Fuji Photo Film Co. Ltd., Tokyo, Japan).

Mutational analysis of the promoter region of *prx*1*ahpF* operon

A pair of primers PRX1-PM01 and -PM02 (Table 2) was designed and used to amplify the 2,470-bp DNA fragment encompassing the *prx*1*ahpF* operon including its promoter region P_{prx}. The PCR product was cloned into the broad-host-range vector pRK415 [14] to create pSS1105 (Table 1). Each of the three nucleotide bases -16T, -8T, and +1G (where +1 is the transcription start site of P_{prx}) within the P_{prx} on pSS1105 was mutated to -16G, -8C, and +1T, respectively (Fig. 3A) using a QuikChange® site-directed mutagenesis kit (Agilent Technologies, Loveland, CO) [19]. The complementary mutagenic primers listed in Table 2 were used in conjunction with the plasmid pSS1105 (as a template DNA) to create pSS1110 (for the -16T→G mutation), pSS1111 (for the -8T→C mutation), and pSS1112 (for the +1G→T mutation) (Table 2). The mutations were confirmed by DNA sequencing. The

pSS1105, pSS1110, pSS1111, or pSS1112 were transferred into the *prx*1 mutant OH0701 (Table 1) by conjugation, and the total RNAs from each strain were subjected to the Northern blot analyses as described above.

Rapid amplification of cDNA 3' ends (3' RACE) assay

The 3' RACE assay to determine 3' end of *prx*1 transcript was performed as described previously [15], with minor modification. Briefly, total cellular RNA (3 μg) from the wild-type *V. vulnificus* grown to an A_{600} of 0.5 after being exposed to 250 μM H_2O_2 for 30 min was dephosphorylated with 0.01 U of calf intestine alkaline phosphatase (New England Biolabs, Ipswich, MA) and then ligated with 500 pmol of 3' adaptor RNA (5'-GCU GAU GGC GAU GAA UGA ACA CUG CUU UGA UGA AA-3') (Bioneer, Seoul, South Korea) with 50 U of T4 RNA ligase (New England Biolabs) in a 50 μl reaction. The adaptor-ligated RNA was reverse-transcribed and amplified with adaptor specific primer RACE-ASP and *prx*1 gene specific primer RACE-GSP (Table 2) using an One-step reverse-transcription PCR (RT-PCR) kit (Qiagen) according to the manufacturer's instructions. The PCR product was separated on 2% agarose gel, purified, and analyzed by DNA sequencing after cloning into the pGEM-T Easy vector.

Construction of P_{prx}-*prx*1*ahpF* intergenic region-*luxCDABE* transcriptional fusions and measurement of cellular luminescence

The 342-bp *prx*1 upstream region extending from −162 to +177, amplified by PCR using a pair of primers PRX1AHPF-01 and -02 (Table 2), was fused with 136 bp of intact *prx*1*ahpF* intergenic region (for pSS1324), amplified by PCR with a pair of primers PRX1AHPF-03 and -04 (Table 2), or with 55 bp of deleted-*prx*1*ahpF* intergenic region (for pSS1326), amplified with a pair of primers PRX1AHPF-03 and -05 (Table 2), using the PCR-mediated linker-

scanning method as described above. As a control, 136-bp DNA fragment within the *prx*1 coding region was amplified by PCR using a pair of primers PRX1-C01 and -C02 (Table 2) and fused with the same *prx*1 upstream region (for pSS1323). Each PCR product was ligated with SacI-SpeI-digested pBBR-*lux* carrying promoterless *luxCDABE* [18] to create pSS reporters (pSS1323, pSS1324, or pSS1326) (Table 2; Fig. 5B) which were then transferred into *V. vulnificus* MO6-24/O by conjugation. The cellular luminescences of the cultures were measured with a luminometer (Lumat model 9507, Berthold, Germany) and expressed in arbitrary relative luminescence unit (RLU), as described previously [13].

Data analyses. Averages and standard errors of the mean (SEM) were calculated from at least three independent experiments. All data were analyzed by Student's *t* tests with the SAS program (SAS software; SAS Institute Inc.). Significance of differences between experimental groups was accepted at a *P* value of < 0.005.

Results and Discussion

The *V. vulnificus prx*1*ahpF* genes are transcribed into two transcripts

The *V. vulnificus ahpF* gene is located downstream of the *prx*1 gene, and the two coding regions of *prx*1 and *ahpF* are transcribed in the same direction with the 136-bp intergenic region (Fig. 1A) [2]. To analyze the transcription pattern of the *V. vulnificus prx*1*ahpF*, Northern blot analyses were performed using the total cellular RNAs isolated from the wild type, the *prx*1 mutant, and the *ahpF* mutant. Since the expression of *prx*1 is known to be induced in cells exposed to high levels of exogenous H_2O_2 [3], the *V. vulnificus* cells were exposed to 250 μM H_2O_2 for 30 min before the RNA isolation. As shown in Fig. 1B, PRX1P probe hybridized to the 0.6 kb RNA corresponding to the *prx*1 transcript when total RNA was isolated from the wild-type cells exposed to 250 μM H_2O_2, reconfirming that the expression of *prx*1 is induced in response to exogenous H_2O_2. In addition, approximately 2.3 kb RNA was detected by PRX1P when the RNA was isolated from the H_2O_2-exposed wild type but not *ahpF* mutant (Fig. 1B). On the basis of the DNA sequence of *prx*1*ahpF*, it was anticipated that a polycistronic *prx*1*ahpF* transcript would be approximately 2.3 kb long (Fig. 1A). Northern blot analysis was performed using AHPFP probe, and a single RNA corresponding to the *prx*1*ahpF* transcript was detected in the RNA isolated from the H_2O_2-exposed wild type but not *ahpF* mutant (Fig. 1C), indicating that the *prx*1*ahpF* genes were also transcribed as a single operon. Therefore, it appeared that the *V. vulnificus prx*1*ahpF* genes transcribed into two transcripts, the high level of *prx*1 transcript and the low level of *prx*1*ahpF* transcript.

The *V. vulnificus prx1ahpF* genes are transcribed from a single promoter

To clarify whether the *prx*1 and *prx*1*ahpF* transcripts are transcribed from each own promoter with different activity or from one promoter, the transcription start site of *prx*1*ahpF* genes

was determined by primer extension analysis. A single transcript was produced from primer extension of RNA isolated from the wild type exposed to 250 μM H_2O_2 (Fig. 2A). The 5' end of the *prx*1 or *prx*1*ahpF* transcript was located 47-bp upstream of the translational initiation codon of *prx*1 and subsequently designated +1 (Fig. 2B). The putative promoter constituting this transcription start site was named P_{prx}. The sequences for the -10 and -35 regions of P_{prx} were assigned on the basis of similarity to consensus sequences of the *E. coli* σ^{70} promoter (Fig. 2B). In addition, the sequences extending from -73 to -37, relative to the transcription start site of P_{prx} (*shaded boxes* in Fig. 2B), showed 87.5% similarity to a consensus sequence of the *E. coli* OxyR-binding site [32], indicating that, consistent with our previous report [16], the *V. vulnificus* OxyR1 may activates the expression of *prx*1*ahpF* by direct binding to the promoter region. Using different sets of primers, no other transcription start sites were identified by primer extension analyses (data not shown). These results suggested that the *prx*1 and *prx*1*ahpF* transcripts are generated from the single promoter, P_{prx}.

To confirm whether the P_{prx} governs the transcription of *prx*1*ahpF in vivo*, three nucleotides of P_{prx}, -16T, -8T, and +1G, which are thought to be important in the transcription, were selected and mutated to -16G, -8C, and +1T, respectively. The DNA fragments encompassing the *prx*1*ahpF* operon with the wild-type and the point-mutated P_{prx} were cloned into pRK415 to create pSS1105, pSS1110, pSS1111, and pSS1112 (Fig. 3A). The activities of each P_{prx} on the pSS1105, pSS1110, pSS1111, and pSS1112 were compared by Northern blot analyses using the RNAs isolated from the each plasmid-containing *prx*1 mutant. Since PRX1P did not detect any transcripts in the RNA isolated from the *prx*1 mutant (Fig. 1B, lane 3), the detected bands in Fig. 3B represent the transcripts which were transcribed from each plasmid. The -16T, a first base of the extended -10 region (normally, TGn) that is recognized by domain 3 of the RNA polymerase σ subunit and the -8T, a fifth base of the -10 region may specify the

initial binding of RNA polymerase to the P_{prx} [4]. As expected, the mutations of -16T to -16G (on pSS1110) and of -8T to -8C (on pSS1111) resulted in the complete abolishment of P_{prx} activity, as determined based on the intensities of the *prx*1 and *prx*1*ahpF* transcripts detected by PRX1P (Fig. 3B). In addition, the mutation of +1G to +1T (on pSS1112) resulted in the increased expression of *prx*1*ahpF* (Fig. 3B), which is possibly attributed to the increased unwinding efficiency of the DNA duplex around the transcription start site of P_{prx} by the mutation. Therefore, these results confirmed that the transcription of *prx*1*ahpF* results in the *prx*1 and *prx*1*ahpF* transcripts from the single promoter which was determined by the primer extension analysis (Fig. 2A).

Stem-loop structure in the *prx*1*ahpF* intergenic region acts as a transcriptional attenuator to create *prx*1 and *prx*1*ahpF* transcripts

There are still two possible ways for the transcription of *prx*1*ahpF* into the two transcripts. One is by degradation of some of the *prx*1*ahpF* transcript through unknown mechanism whereas another is by transcriptional attenuation at the intergenic region of *prx*1*ahpF*, resulting in the high level of *prx*1 transcript and the low level of *prx*1*ahpF* transcript. In the Northern blot analysis, however, the *prx*1 transcript still detected by PRX1P in the RNA isolated from the *ahpF* mutant that cannot produce the *prx*1*ahpF* transcript (Fig. 1B, lane 4), therefore the former hypothesis is not the case. To verify the latter hypothesis, we first examined whether there is any transcriptional termination site within the *prx*1*ahpF* intergenic region using 3' RACE assay. Total RNA isolated from the wild type exposed to 250 μM H_2O_2 was ligated to a 3' adaptor, followed by RT-PCR amplification, and the resulting PCR products were then analyzed on an agarose gel. As a result, only one band was detected at comparable levels (Fig. 4A) and was then eluted from the gel and subjected to the DNA sequencing analysis (Table 3). The sequencing data suggested that the band was derived from

the *prx*1 transcript with 3' end, +689T, located 83-bp downstream of the translational stop codon of *prx*1 as indicated in Fig. 4B. These results suggested that the transcription of *prx*1*ahpF* can be terminated at the intergenic region to result in the *prx*1 transcript.

Possible mechanism of the transcriptional termination at the intergenic region of *prx*1*ahpF* was further investigated by predicting the secondary structure of the RNA deduced from the 137-bp intergenic region DNA. As a result, a stem-loop structure comprising of 49 bp RNA with an 18 base pair-stem formed by a palindrome region and a 13 bases-loop was singled out (Fig. 4C). The stem-loop structure was followed by a stretch of cytosine residues (CCCC) and the 3' end of *prx*1 transcript (U), which is likely to serve as a rho-independent intrinsic terminator of transcription. The canonical intrinsic terminator of *E. coli* is known to include a poly(U) tract following a palindrome on the transcript [24], and the poly(U) tract is known to contribute to the termination of transcription by reducing the stability the RNA-DNA hybrid [17]. Therefore, it is highly intriguing that the putative terminator in the *prx*1*ahpF* intergenic region has no poly(U) tract after the stem-loop structure (Fig. 4C).

It has been reported that disruption of the poly(U) tract of intrinsic terminator reduces its transcriptional termination activity significantly but not completely [1]. Therefore, it is reasonable to hypothesize that the putative atypical terminator in the *prx*1*ahpF* intergenic region attenuates the transcription of *prx*1*ahpF* by not having the poly(U) tract, leading to the production of the high level of *prx*1 transcript and the low level of *prx*1*ahpF* transcript. In order to experimentally verify this hypothesis, the P_{prx} ligated with the 136 bp of intact intergenic region or the 55 bp of deleted intergenic region, in which the downstream half of the palindrome was deleted, was fused with the *luxCDABE* reporter genes (Fig. 5A). Culture luminescene was used to quantify the capacity of each intergenic region to terminate

transcription (Fig. 5B). The RLU of pSS1324 carrying the intact intergenic region was about 6-fold lower than that of pSS1323 carrying the DNA fragment from the *prx*1 coding region used as a control, indicating that the *prx*1*ahpF* intergenic region is indeed important for the transcriptional termination. For pSS1326 carrying the deleted intergenic region which could not form the stem-loop structure, the RLU was about 8-fold higher compared to pSS1323. This result suggested that the stem-loop structure is indispensable for the transcriptional termination. It is noteworthy that, although pSS1324 contained the intact stem-loop structure, its RLU was a considerable quantity of 1.0×10^4, not fully abolished, implying that the stem-loop structure did not completely terminate the transcription to produce the low level of *prx*1*ahpF* transcript. Therefore, it was proved that the stem-loop structure functions as the attenuator of *prx*1*ahpF* transcription, which leads to the co-production of high level of *prx*1 transcript and low level of *prx*1*ahpF* transcript.

Differential expression of *prx*1 and *prx*1*ahpF* transcripts by the *cis*-acting intrinsic terminator, which leads to the production of high level of Prx1 and low level of AhpF could have considerable benefits. First, intrinsic terminator, an ancient regulatory mechanism, that does not require any additional factors for its activity is largely economic and efficient [24]. Second, the ratio of the amount of cellular Prx1 and AhpF proteins resulted from the controlled expression by the terminator can be maintained stably regardless of environmental conditions that bacteria can encounter. This is noticeable because the high production of AhpF, the NADH-consuming protein, more than needs could cause disruption of the intracellular NADH homeostasis. Therefore, the quantitative control of AhpF may be important to avoid unnecessary loss of NADH and inappropriate flow of electrons in the cell. Consistent with this, it has been reported that *E. coli* cells overexpressing *Pseudomonas putida ahpF* were more sensitive to oxidants such as H_2O_2 and *tert*-butyl hydroperoxide [9].

In summary, our data presented here extended our understanding of the transcription of *V. vulnificus prx*1*ahpF* by demonstrating that the *prx*1*ahpF* genes are transcribed from a single promoter to produce both *prx*1 and *prx*1*ahpF* transcripts by the intergenic stem-loop structure-mediated transcriptional attenuation. The resulting precisely controlled expression of Prx1 and AhpF may be crucial for maintaining the NADH homeostasis of *V. vulnificus* and thereby further contribute to ROS-scavenging activity of the pathogen under oxidative stress.

Footnotes

Author contributions: Hyun Sung Lee and Jong Gyu Lim contributed equally to this work.

Acknowledgement

This work was supported by a grant from the Public Welfare and Safety Research Program (2012M3A2A1051679) and a grant from Mid-career Research Program (2010-0029167) through the National Research Foundation funded by the Ministry of Science, ICT, and Future Planning, and a grant (14162MFDS972) from the Ministry of Food and Drug Safety, Republic of Korea.

References

1. Abe H, Aiba H. 1996. Differential contributions of two elements of rho-independent terminator to transcription termination and mRNA stabilization. *Biochimie* **78:** 1035-1042.
2. Baek WK, Lee HS, Oh MH, Koh MJ, Kim K, Choi SH. 2009. Identification of the *Vibrio vulnificus ahpC*1 gene and its influence on survival under oxidative stress and virulence. *J. Microbiol.* **47:** 624-632.
3. Bang YJ, Oh MH, Choi SH. 2012. Distinct characteristics of two 2-Cys peroxiredoxins of *Vibrio vulnificus* suggesting differential roles in detoxifying oxidative stress. *J. Biol. Chem.* **287:** 42516-42524.
4. Browning DF, Busby SJ. 2004. The regulation of bacterial transcription initiation. *Nat. Rev. Microbiol.* **2:** 57-65.
5. Christman MF, Morgan RW, Jacobson FS, Ames BN. 1985. Positive control of a regulon for defenses against oxidative stress and some heat-shock proteins in *Salmonella typhimurium*. *Cell* **41:** 753-762.
6. Dubbs JM, Mongkolsuk S. 2007. Peroxiredoxins in bacterial antioxidant defense. *Subcell. Biochem.* **44:** 143-193.
7. Dubbs JM, Mongkolsuk S. 2012. Peroxide-sensing transcriptional regulators in bacteria. *J. Bacteriol.* **194:** 5495-5503.
8. Fang FC. 2004. Antimicrobial reactive oxygen and nitrogen species: concepts and controversies. *Nat. Rev. Microbiol.* **2:** 820-832.
9. Fukumori F, Kishii M. 2001. Molecular cloning and transcriptional analysis of the alkyl hydroperoxide reductase genes from *Pseudomonas putida* KT2442. *J. Gen. Appl. Microbiol.* **47:** 269-277.
10. Hall A, Karplus PA, Poole LB. 2009. Typical 2-Cys peroxiredoxins-structures,

mechanisms and functions. *FEBS J.* **276:** 2469-2477.

11. Imlay JA. 2008. Cellular defenses against superoxide and hydrogen peroxide. *Annu. Rev. Biochem.* **77:** 755-776.
12. Jacobson FS, Morgan RW, Christman MF, Ames BN. 1989. An alkyl hydroperoxide reductase from *Salmonella typhimurium* involved in the defense of DNA against oxidative damage. *J. Biol. Chem.* **264:** 1488-1496.
13. Jeong HS, Kim SM, Lim MS, Kim KS, Choi SH. 2010. Direct interaction between quorum-sensing regulator SmcR and RNA polymerase is mediated by integration host factor to activate *vvpE* encoding elastase in *Vibrio vulnificus*. *J. Biol. Chem.* **285:** 9357-9366.
14. Keen NT, Tamaki S, Kobayashi D, Trollinger D. 1988. Improved broad host-range plasmids for DNA cloning in Gram-negative bacteria. *Gene* **70:** 191-197.
15. Kim KS, Lee Y. 2004. Regulation of 6S RNA biogenesis by switching utilization of both sigma factors and endoribonucleases. *Nucleic acids Res.* **32:** 6057-6068.
16. Kim S, Bang YJ, Kim D, Lim JG, Oh MH, Choi SH. 2014. Distinct characteristics of OxyR2, a new OxyR-type regulator, ensuring expression of Peroxiredoxin 2 detoxifying low levels of hydrogen peroxide in *Vibrio vulnificus*. *Mol. Microbiol.* **93:** 992-1009.
17. Komissarova N, Becker J, Solter S, Kireeva M, Kashlev M. 2002. Shortening of RNA: DNA hybrid in the elongation complex of RNA polymerase is a prerequisite for transcription termination. *Mol. cell* **10:** 1151-1162.
18. Lenz DH, Mok KC, Lilley BN, Kulkarni RV, Wingreen NS, Bassler BL. 2004. The small RNA chaperone Hfq and multiple small RNAs control quorum sensing in *Vibrio harveyi* and *Vibrio cholera*. *Cell* **118:** 69-82.
19. Lim JG, Bang YJ, Choi SH. 2014. Characterization of the *Vibrio vulnificus* 1-Cys peroxiredoxin Prx3 and regulation of its expression by the Fe-S cluster regulator IscR in

response to oxidative stress and iron starvation. *J. Biol. Chem.* **289:** 36263-36274.

20. Markham NR, Zuker M. 2008. UNAFold: Software for nucleic acid folding and hybridization. pp. 3-31. *In* Keith JM (ed), *Bioinformatics: Structure, functions and applications*, Vol. 453, Humana Press, Totowa, NJ.
21. Miller RA, Britigan BE. 1997. Role of oxidants in microbial pathophysiology. *Clin. Microbiol. Rev.* **10:** 1-18.
22. Miller VL, Mekalanos JJ. 1988. A novel suicide vector and its use in construction of insertion mutations: osmoregulation of outer membrane proteins and virulence determinants in *Vibrio cholerae* requires *toxR*. *J. Bacteriol.* **170:** 2575-2583.
23. Milton DL, O'Toole R, Horstedt P, Wolf-Watz H. 1996. Flagellin A is essential for the virulence of *Vibrio anguillarum*. *J. Bacteriol.* **178:** 1310-1319.
24. Mitra A, Angamuthu K, Jayashree HV, Nagaraja V. 2009. Occurrence, divergence and evolution of intrinsic terminators across Eubacteria. *Genomics* **94:** 110-116.
25. Nathan C, Shiloh MU. 2000. Reactive oxygen and nitrogen intermediates in the relationship between mammalian hosts and microbial pathogens. *Proc. Natl. Acad. Sci. U.S.A.* **97:** 8841-8848.
26. Oka A, Sugisaki H, Takanami M. 1981. Nucleotide sequence of the kanamycin resistance transposon Tn903. *J. Mol. Biol.* **147:** 217-226.
27. Poole LB, Hall A, Nelson KJ. 2011. Overview of peroxiredoxins in oxidant defense and redox regulation. *Curr. Protoc. Toxicol.* **49:** 7.9.1-7.9.15.
28. Sambrook J, Russell D. 2001. *Molecular Cloning: A Laboratory Manual*, 3rd Ed. Cold Spring Harbor laboratory Press, New York.
29. Storz G, Imlay JA. 1999. Oxidative stress. *Curr. Opin. Microbiol.* **2:** 188-194.
30. Storz G, Jacobson F, Tartaglia L, Morgan R, Silveira L, Ames B. 1989. An alkyl hydroperoxide reductase induced by oxidative stress in *Salmonella typhimurium* and

Escherichia coli: genetic characterization and cloning of *ahp*. *J. Bacteriol.* **171:** 2049-2055.

31. Storz G, Zheng M. 2000. *Bacterial Stress Responses*, pp. 47-59. *In* Storz G, Hengge-Aronis R (eds), pp. 47-59. ASM Press, Washington, D. C.
32. Toledano MB, Kullik I, Trinh F, Baird PT, Schneider TD, Storz G. 1994. Redox-dependent shift of OxyR-DNA contacts along an extended DNA-binding site: a mechanism for differential promoter selection. *Cell* **78:** 897-909.

Fig. 1. Genetic organization and transcript analysis of *V. vulnificus prx*1*ahpF*.

(A) The *shaded arrows* represent the transcriptional directions and the coding regions of the *V. vulnificus prx*1 (VVMO6_03966) and *ahpF* (VVMO6_03967). Locus tag numbers based on the database of the *V. vulnificus* MO6-24/O genome sequence (GenBank accession numbers CP002469 and CP002470) are shown above each coding region. The DNA probes, PRX1P and AHPFP, used for Northern blot analyses are depicted below each coding region by *shaded bars*. (B and C) Total RNAs were isolated from the strains grown to an A_{600} of 0.5 after being exposed to 250 μM H_2O_2 for 30 min as indicated. RNAs were resolved and hybridized to a ^{32}P-labeled DNA probe corresponding to the internal coding regions of *prx*1 (PRX1P, B) or *ahpF* (AHPFP, C). The RNA size markers (Invitrogen) and *prx*1 and *prx*1*ahpF* transcripts are shown in kilobases. *prx*1, *prx*1 mutant; *ahpF*, *ahpF* mutant.

Fig. 2. Transcription start sites and sequence analysis of the *prx*1*ahpF* promoter region.

(A) Transcription start site of P_{prx}, indicated by the *asterisk*, was determined by primer extension of the RNA derived from the wild-type *V. vulnificus* grown to an A_{600} of 0.5 after being exposed to 250 μM H_2O_2 for 30 min. *Lanes C, T, A,* and *G* represent the nucleotide sequencing ladders of pSS1050. (B) The transcription start site of P_{prx} (+1) is indicated by a *bent arrow* and the positions of the putative -10 and -35 regions are *underlined*. The putative sequences for binding of OxyR1 are presented as *shaded boxes*. The consensus sequences of the *E. coli* OxyR-binding site are indicated above the *V. vulnificus* DNA sequence. The ATG translation initiation codons and the putative ribosome-binding site (*SD*) are also shown in *boldface*.

Fig. 3. Effect of the P_{prx} mutation on the *prx*1*ahpF* transcription.

(A) A set of DNA fragments encompassing the wild-type or mutated P_{prx} and the *prx*1*ahpF*

operon were subcloned into pRK415 to create pSS1105, pSS1110, pSS1111, or pSS1112 for Northern blot analyses as shown in *shaded box*. The transcription start site of P_{prx} (+1) and the putative -10 and extended -10 (TGn) regions are *underlined*. (B) Total RNAs were isolated from the exponential phase culture (A_{600} = 0.5) of the *prx*1 mutant containing each plasmid and then resolved and hybridized to PRX1P. The results are presented as described in Fig. 1B.

Fig. 4. Determination of the 3'end of *prx*1 transcript and sequence analysis of the *prx*1*ahpF* intergenic region.

(A) The 3' RACE product of the RNA derived from the wild-type *V. vulnificus* grown to an A_{600} of 0.5 after being exposed to 250 μM H_2O_2 for 30 min was separated on a 2% agarose gel and indicated by *an arrow*. The DNA size markers (100-bp DNA ladder, New England Biolabs) are shown in kilobases. (B) The coding regions of *prx*1*ahpF* genes and the chromosomal DNA are indicated by *arrow boxes* and *a thick line* respectively. DNA sequences of the 136-bp *prx*1*ahpF* intergenic region indicated by *a black box* are shown. The 3' end position of the *prx*1 transcript (T) that is determined by 3' RACE assay (Table 3), the translational stop codon of *prx*1 (TAA) and the translational initiation codon of *ahpF* (ATG) are indicated in *boldface*. *Black arrows* indicate a palindrome in the *prx*1*ahpF* intergenic region. (C) The RNA secondary structure of the RNA deduced from the 56-bp DNA sequence indicated by *a shaded box* in panel B was predicted by the UNAfold software [20] (http://www.bioinfo.rpi.edu/applications/mfold/).

Fig. 5. Deletion analysis of the *prx*1*ahpF* intergenic region.

(A) P_{prx}-*prx*1*ahpF* intergenic region-*luxCDABE* transcriptional fusion pSS reporters were created as described in 'Materials and Methods'. The promoter region (P_{prx}) and intergenic region of *prx*1*ahpF* are indicated by *dark gray boxes* and *black boxes* respectively. *Lollipops*

on the black boxes represent the stem-loop structure between the two genes, predicted in Fig. 4C. The 136-bp DNA fragment within the coding region of *prx*1 used as a positive control (for pSS1323) is presented as *a dotted box*. (B) Cellular luminescences were determined from the log phase culture (A_{600} = 0.5) of *V. vulnificus* containing each pSS reporter as indicated. Error bars represent the SEM. **, $P < 0.005$ relative to the *V. vulnificus* containing pSS1324.

Table 1. Plasmids and bacterial strains used in this study

Strain or plasmid	Relevant characteristics [a]	Reference or source
Bacterial Strains		
V. vulnificus		
MO6-24/O	Clinical isolate; virulent	Laboratory collection
OH0701	MO6-24/O with *prx*1::*nptI*; Km^r	[2]
BK081	MO6-24/O with *ahpF*::*nptI*; Km^r	This study
E. coli		
DH5α	λ^- ϕ80d*lacZ*ΔM15 Δ(*lacZYA-argF*)*U169 recA1 endA1 hsdR17* (r_K^- m_K^-) *supE44 thi-1 gyrA relA1*; plasmid replication	Laboratory collection
SM10 λ *pir*	λ-*pir* lysogen; *thi thr leu tonA lacY supE recA*::RP4-2-Tc::Mu λ *pir*; Km^r host for π-requiring plasmids; conjugal donor	[22]
Plasmids		
pDM4	R6K γ *ori sacB*; suicide vector; *oriT* of RP4; Cm^r	[23]
pWK0805	pDM4 with *ahpF*::*nptI*; Cm^r, Km^r	This study
pGEM-T Easy	PCR product cloning vector; Ap^r	Promega
pSS1050	pGEM-T Easy with a 410-bp DNA fragment of the putative promoter region of *prx*1	This study
pRK415	Inc P *ori*; broad host range vector; *oriT* of RP4; Tc^r	[14]
pSS1105	pRK415 with P_{prx} and *prx*1*ahpF* operon; Tc^r	This study
pSS1110	pSS1105 with mutation (-16T→G)[b] in P_{prx}; Tc^r	This study
pSS1111	pSS1105 with mutation (-8T→C)[b] in P_{prx}; Tc^r	This study
pSS1112	pSS1105 with mutation (+1G→T)[b] in P_{prx}; Tc^r	This study
pBBR-*lux*	Broad host range vector containing promoterless *luxCDABE*; Cm^r	[18]
pSS1323	pBBR-*lux* with P_{prx} and 136-bp DNA fragment of *prx*1 coding region	This study
pSS1324	pBBR-*lux* with P_{prx} and 136-bp DNA fragment of *prx*1*ahpF* intergenic region	This study
pSS1326	pBBR-*lux* with P_{prx} and 55-bp DNA fragment of *prx*1*ahpF* intergenic region	This study

[a] Km^r, kanamycin-resistant; Cm^r, chloramphenicol-resistant; Ap^r, ampicillin-resistant; Tc^r, tetracycline-resistant.

[b] Shown are the nucleotide positions within the P_{prx}, where +1 is the transcription start site of P_{prx}.

Table 2. Oligonucleotides used in this study

Name	Oligonucleotide Sequence (5' → 3')[a, b]	Use
For mutant construction		
AHPF0801	GAATTTACATCCTTAGTTCTTGCCC	Construction of *ahpF* mutant
AHPF0802	CATGGGATCCATCACCTGACCA	
AHPF0803	TGGTCAGGTGATGGATCCCATG	
AHPF0804	AAGCCAGTCACACGTTTACCATCAC	
For Northern blot analysis		
PRX1-NB01	CGACTGAACTTGGTGACCTAGCAGACC	PRX1P DNA probe
PRX1-NB02	TTGCGTAGTAGGTCTTCTGCGTCACG	
AHPF-NB01	CACACTGTGATGGCCCTTTGT	AHPFP DNA probe
AHPF-NB02	TACCATCACCAACCACTTCGG	
For primer extension analysis		
PRX1-PE01	CAAACTGGTTGGCAAATCAGCCGT	Amplification of *prx*1 upstream region
PRX1-PE02	CATTTGCCCAATACGTCTTGTTC	Amplification of *prx*1 upstream region, Extension of *prx*1 transcript
For mutagenesis of *prx*1 upstream region		
PRX1-PM01	AAAAGAGCTCCACAACGCTATCACAC	Amplification of the DNA fragment encompassing P_{prx} and *prx*1*ahpF* operon
PRX1-PM02	GGTTAAGCTTAGCCTTGCTTACGAATCAAGTAA	
PRX1-PM03	CGGGAGGTATATTCACCTTCTGACCC	-16T→G[c] mutation in P_{prx}
PRX1-PM04	GGGTCAGAAGGTGAATATACCTCCCG	
PRX1-PM05	CGGGAGGTGTATTCACATTCTGACC	-8T→C[c] mutation in P_{prx}
PRX1-PM06	GGTCAGAATGTGAATACACCTCCCG	
PRX1-PM07	CGCTTGCCTTAGGGAGGTATATTCAC	+1G→T[c] mutation in P_{prx}
PRX1-PM08	GTGAATATACCTCCCTAAGGCAAGCG	
For 3' RACE assay		
RACE-ASP	CAAAGCAGTGTTCATTCATCGCC	3' adaptor RNA specific primer
RACE-GSP	CAACTGACACGCATTTC	*prx*1 gene specific primer
For deletion assay of *prx*1*ahpF* intergenic region		
PRX1AHPF-01	AAAAGAGCTCCACAACGCTATCACAC	Amplification of *prx*1 upstream region
PRX1AHPF-02	GACTCAGATCCGAAAGTGAAGTCCGCTG	
PRX1AHPF-03	GATCTGAGTCTCATTTGCGTTGATTACCC	Amplification of *prx*1*ahpF* intergenic region
PRX1AHPF-04	GCTTGGTCACTAGTACTCGAATACCTTTATAGTTT	
PRX1AHPF-05	AGCATTACTAGTGTCAAGTAAAACGCCCG	
PRX1-C01	GATCTGAGTCAACTGACACGCATTTC	Amplification of a part of the *prx*1 coding region
PRX1-C02	CACGGACTAGTAGACCTTGGCCTGGG	

[a] The oligonucleotides were designed using the *V. vulnificus* MO6-24/O genomic sequence (GenBank™ accession number CP002469 and CP002470, www.ncbi.nlm.nih.gov).

[b] Regions of oligonucleotides not complementary to the corresponding genes are underlined.

[c] Shown are the nucleotide positions within the P_{prx}, where +1 is the transcription start site of P_{prx}.

Table 3. Sequencing analysis of the 3' RACE products

3' ends of *prx*1 transcript[a]
+644[b] (1)[c], +658 (3), +664(1), +687 (1), +689 (8), +695 (1), +708 (1)

[a] The RACE products shown in Fig. 4A were cloned into pGEM-T Easy vector and analyzed by DNA sequencing.

[b] Shown are the nucleotide positions within the P_{prx}, where +1 is the transcription start site of P_{prx}.

[c] The numbers in parentheses indicate the frequency of occurrence.

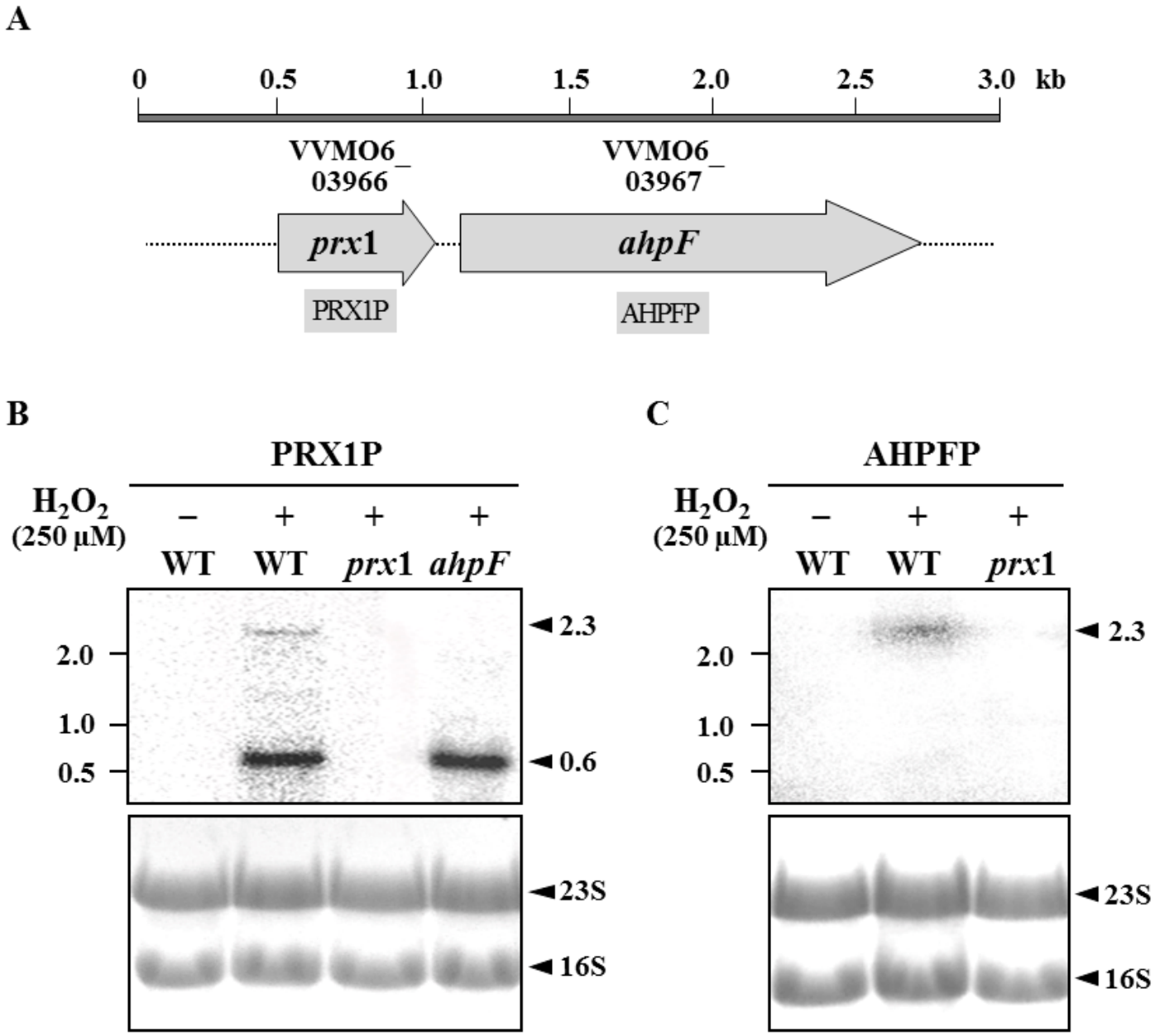
A
0
0.5
1.0
1.5
2.0
2.5
3.0
kb
VVMO6_
03966
VVMO6_
03967
prx1
ahpF
PRX1P
AHPFP
B
PRX1P
H2O2
(250 μM)
–
+
+
+
WT
WT
prx1
ahpF
2.0
1.0
0.5
2.3
0.6
23S
16S
C
AHPFP
H2O2
(250 μM)
–
+
+
WT
WT
prx1
2.0
1.0
0.5
2.3
23S
16S

Fig. 1

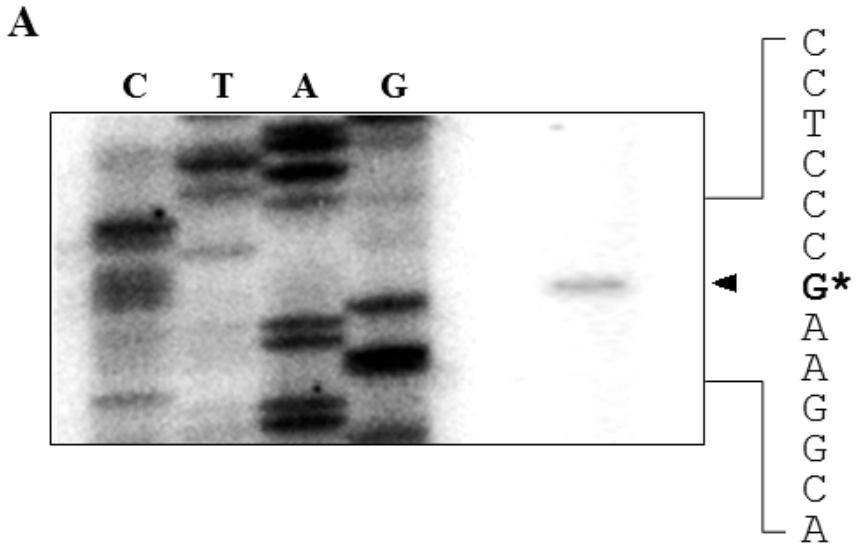

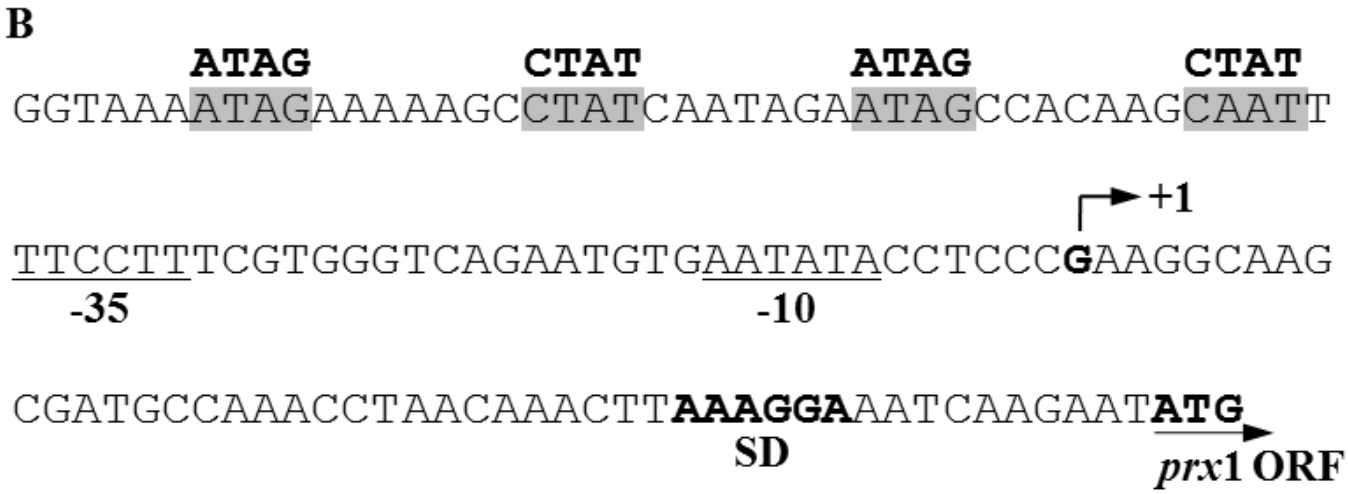

Fig. 2

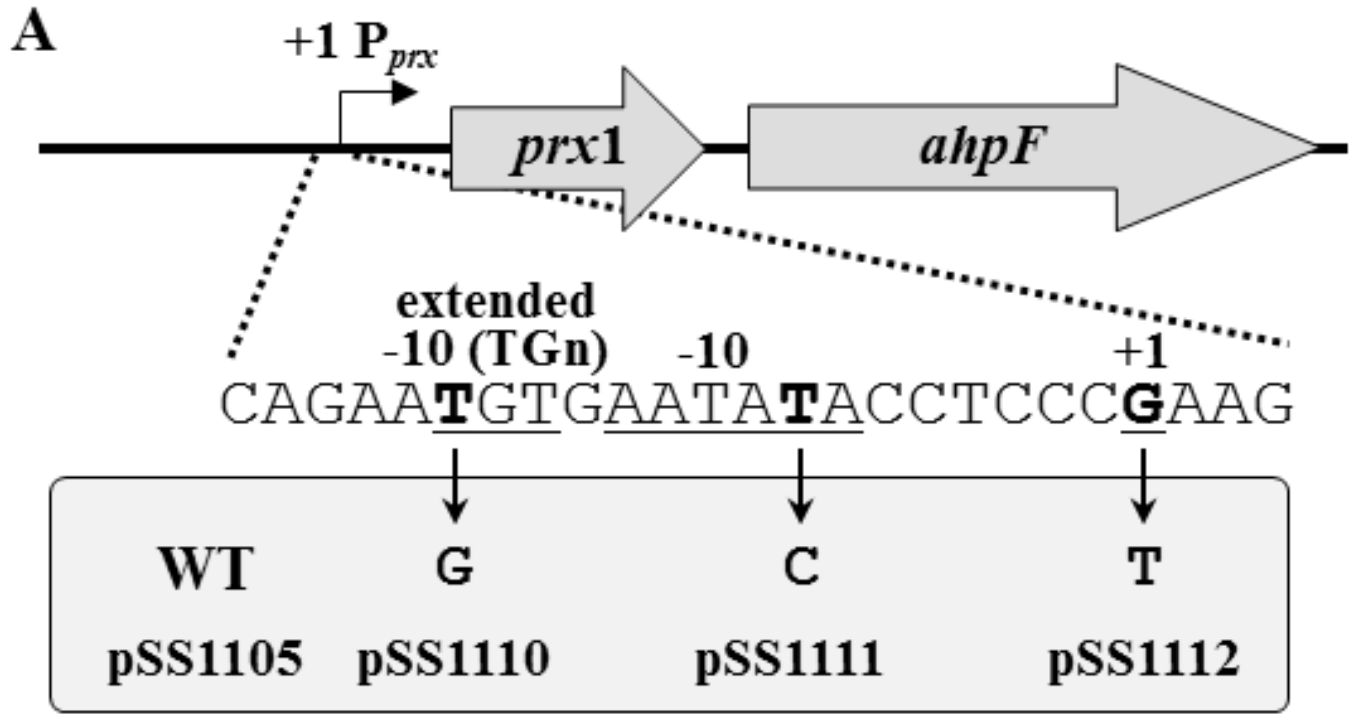
A
+1 P prx
prx1
ahpF
extended
-10 (TGn)
-10
+1
CAGAATGTGAATATACCTCCCGAAG
WT
G
C
T
pSS1105
pSS1110
pSS1111
pSS1112

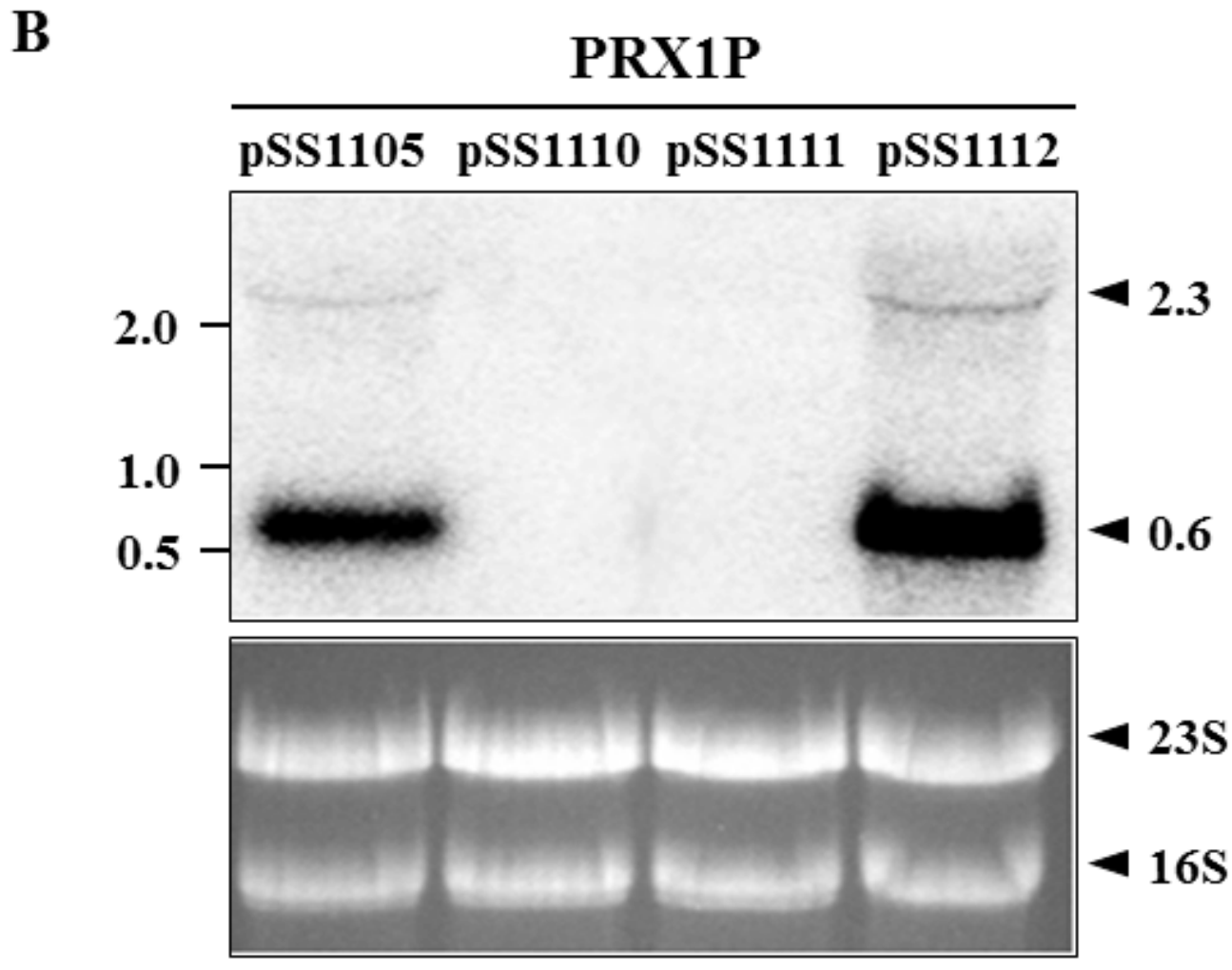
B
PRX1P
pSS1105
pSS1110
pSS1111
pSS1112
2.0
1.0
0.5
2.3
0.6
23S
16S

Fig. 3

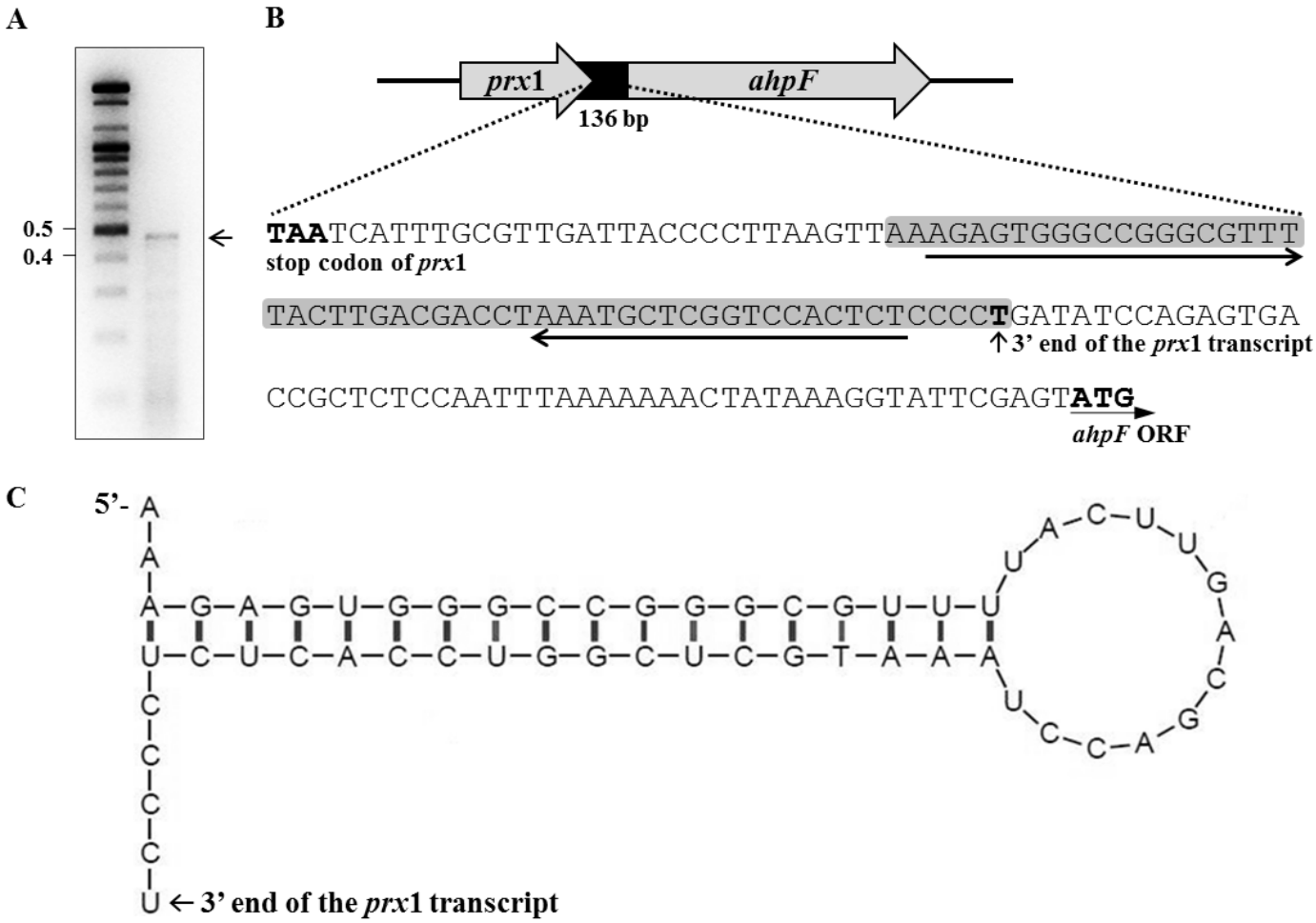

Fig. 4

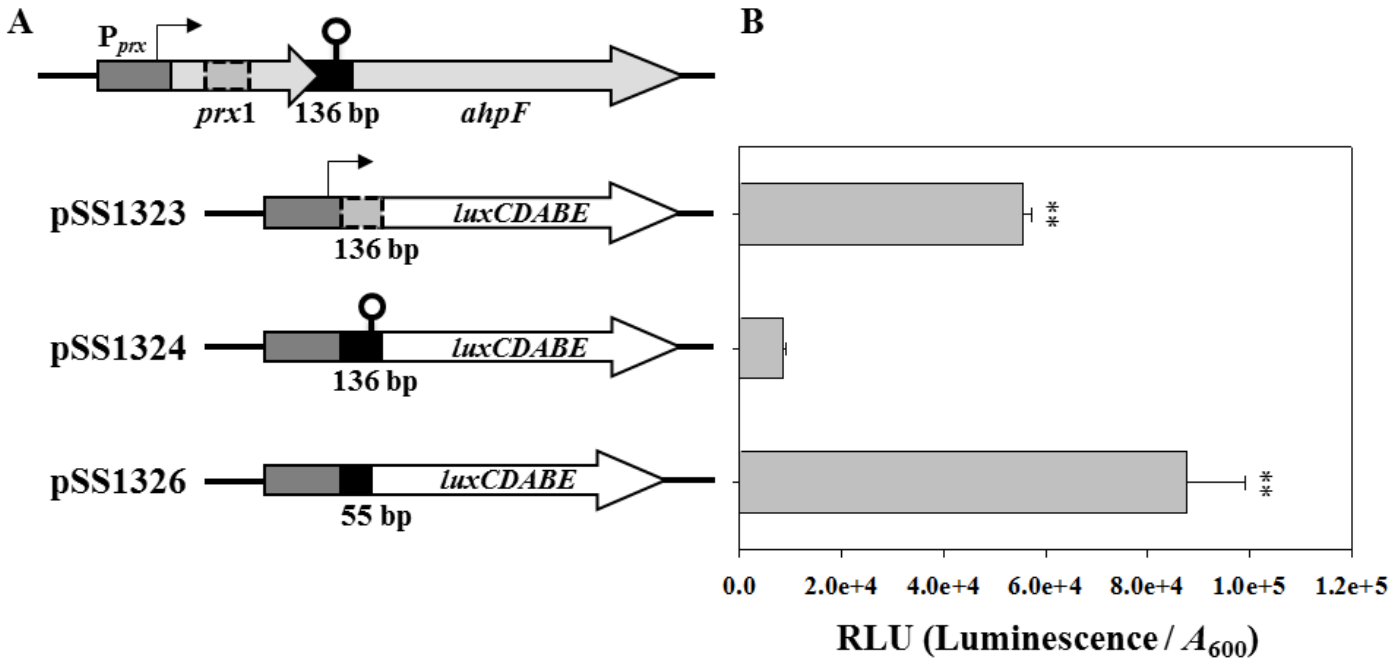
A
B
P prx
prx1
136 bp
ahpF
pSS1323
luxCDABE
136 bp
pSS1324
luxCDABE
136 bp
pSS1326
luxCDABE
55 bp
**
**
0.0
2.0e+4
4.0e+4
6.0e+4
8.0e+4
1.0e+5
1.2e+5
RLU (Luminescence / A600)

Fig. 5